International Journal of Physics
and Research (IJPR)
ISSN (P): 2250–0030; ISSN (E): 2319–4499
Vol. 9, Issue 2, Dec 2019, 7–22

TRANS STELLAR
•Journal Publications •Research Consultancy

THE EFFECT OF EU^{3+} AND ALKALINE EARTH IONS ON THE SPECTROSCOPIC AND FLUORESCENCE PROPERTIES OF ZINC BORATE GLASS FOR ACTIVE PHOTONIC APPLICATIONS

D. VIJAYA SRI[1] & CH. LINGA RAJU[2]

[1]*T. R. R. Government Degree College, Kandukur, Prakasam District, Andhra Pradesh, India*

[2]*Department of Physics, Acharya Nagarjuna University, N. Nagar, Andhra Pradesh, India*

ABSTRACT

Zinc containing alkaline earth borate glasses doped with trivalent Eu^{3+}ions were prepared and characterized. The influence of host composition ions on the borate structure was analyzed through FTIR spectroscopy. From the absorption spectrum, the J-O intensity parameters reveal the double bond nature of Eu-O bonds in present glass matrix. Her adiative properties for the transition $^5D_0 \rightarrow ^7F_J$have been calculated with J-O and emission measurements. In the present glass, the Ω_2 parameter indicate she good polarizable chemical domain situated on every side of the Eu^{3+} ions. The results confirm the probability of existing Eu^{3+} doped MZB glasses as laser active substances to fabricate a bright red fluorescence at 612 nm due to $^5D_0 \rightarrow ^7F_2$ emission transition, which is also confirm through CIE color coordinate diagram.

KEYWORDS: Alkaline Earth and Eu^{3+} Ions, Optical Studies, Oscillator Strengths, J-O parameters & Photo-Luminescence

Received: Jun 17, 2019; **Accepted:** Jul 12, 2019; **Published:** Aug 21, 2019; **Paper Id.:** IJPRDEC20192

Original Article

INTRODUCTION

Multiple chemical compositions of glass matrix influence optical properties, which in turn changes radiative properties [1]. The novel and significant optical characteristics of Ln^{3+} ions doped oxide glasses act as prominent materials in photonics. The unique applications of photonics led to the developments in electro optics, opt mechanics and quantum electronics [2].

Oxides are suitable materials for preparing the efficient luminescence in rare earth ions [3]. Borate based glasses are best for such luminescence host material purpose, which clearly shows the variations in its structural properties with alkaline earth cations [4]. Most of the oxide glasses with the alkali content show, non-linear behavior. This arises depending on the static structure and origination of non-bridging oxygen with alkaline earth ions in the system [5]. It has much importance in understanding the movement of ions in glasses. Alkaline earth oxides own high conductivity than other heavy metal oxides, and hence act as good ionic conductor [6]. Previous studies confirmed that alkaline earth oxides suppressed the hygroscopic quality of borate glass and improve the glass forming nature [2, 6, 7].

Zinc oxide is considered as a good material host for RE doped systems, as it has a broad band gap and considerable binding energy in the vicinity of room temperature [8]. The properties of zinc oxide can be significantly improved by doping impurities. The rare earth doped zinc oxide properties are related to the trivalent electronic structure of RE^{3+}, which mainly depends on the optical 4f – 4f transitions. A glass including heavy metal

oxides shows desired non-linear properties and chemical durability. Zinc oxide shows considerable applications in electronics due to simultaneous observation of intense ultraviolet and visible emissions in white light-emitting devices. When the divalent cation (zinc) is injected in large composition compared to alkaline earth metal oxides, it is found as network modifier and the oxygen becomes non-bridging. So zinc oxide with good electro-optic properties is the best host for electronic materials [9].

Pure boron trioxide (B_2O_3) is covalently bonded, with unique structural features. The structural change between BO_3 and BO_4 results the compactness of glass structure. It forms a random network with non-bridging oxygen, accommodating more number of RE ions. The selection of borate glass systems are due to its good ionic conducting nature, low melting temperature, high thermal stability and high transparency with rare earth do pant [10,11].

Now days, research is much focused on rare earth doped glasses not only in infrared, but also in visible optical device. Among Ln^{3+} ions, the europium ion (Eu^{3+}) has been studied widely due to their easily understood energy level configuration, also sensitivity of fluorescence on the environment [12]. So the selection of aeuropium ion is best for development of red emitting phosphor for field emission technology because of the narrow and monochromatic nature of the $^7F_0 \rightarrow {}^5D_2$ emission. It exhibits pure magnetic & electric dipole transitions as probe to find the structural variation. The probability of the magnetic dipole transitions ($^7F_0 \rightarrow {}^5D_1$) is not influenced by the environment, but the hypersensitive transition ($^7F_0 \rightarrow {}^5D_2$) is depressed under a higher symmetric environment. Oxide glasses are suitable hosts to study the structural variations around the RE ions and to increase the efficiency of the luminescence properties. To know the effect of the chemical environment on rare earth ions, glasses are best as hosts and for efficient luminescence, oxide glass hosts are good [2]. The modifiers, M^{2+} and Zn^{2+}oxides improve the luminescence intensity and increase the strength regarding the glass network [13]. Europium oxide as an activator, used to enhance the luminescence properties. Finally, a host of borate rich glasses, along with M^{2+} and Zn^{2+}oxides as glass modifiers doped with Eu^{3+}ions, are promising candidates for their probable applications in optical fibers, optical filters, laser hosts, γ-ray absorbers, photonic devices, etc. [14].

Our work is to investigate the spectroscopic characteristics of Eu^{3+} doped zinc borate glasses, embedded with alkaline earth metals by using various versatile analytical techniques like XRD, FTIR, optical, photo-luminescence and the lifetime measurements.

EXPERIMENTAL

The present glass system is represented as $10MO\text{-}(30\text{-}x)ZnO\text{-}60B_2O_3\text{-}xEu_2O_3$ (where M=Ca, Sr, Ba and x=1,2,3 mol%) with appropriate high purity (99.99%) analytical grade chemicals of H_3BO_3, ZnO, BaO, CaO, SrO, Eu_2O_3 and were prepared by conventional melt quenching technique with the molar percentages as listed in the Table 1. (Hereafter, europium doped alkaline earth zinc borate glasses are referred as Eu^{3+}: MZB).

Table 1: Chemical Compositions of Eu3+ (mol %) Doped MZB Glasses

Glass Composition	M-O	ZnO	B2O3	Eu2O3
MZB: Eu3+ (Pure)	10	30	60	----
CZB: Eu3+ (1 mol %)	10	29	60	1
BZB: Eu3+ (1 mol %)	10	29	60	1
SZB: Eu3+ (1 mol %)	10	29	60	1
SZB: Eu3+ (2 mol %)	10	28	60	2
SZB: Eu3+ (3 mol %)	10	27	60	3

About 5 batches of 15 grams of each system were weighed accurately and thoroughly mixed in an agate mortar to attain homogeneity and the powder is taken in a silica crucible, melted in the furnace at a temperature of 1150 ^{0}C for 45 min. The melts were air quenched by pouring them on a preheated brass plate. Now, the glass samples annealed at 400 ^{0}C for 4 hours to remove thermal and internal strains. Prepared glasses were polished for optical studies.

Characterization

Physical properties like density and refractive index were measured by the standard Archimedes method using O-Xylene as an immersion liquid and Abbe's refractometer at sodium wavelength with 1-bromo naphthalene as a contact liquid, respectively.

The amorphous nature of prepared glass is confirmed through XRD technique at room temperature and FTIR spectra were recorded using JASCO-FTIR-6200 spectrometer in the range 400-2000 cm^{-1} using KBr pellet technique. Using Hitachi U-3400 UV-VIS spectrophotometer, optical absorption spectra was recorded in the wavelength region 350–2400 nm. The excitation & emission spectra were recorded with the help of Hitachi 650-10 s fluorescence photo spectrometer. The Lifetime of the $^4G_{5/2}$ excited level for different glass compositions with 402 nm excitation wavelength are measured.

RESULTS AND DISCUSSIONS

Physical Parameters

The variables like density, molar volume, refractive index and an optical band gap were measured and calculated. The parameters like europium-ion concentration, polar on radius, polarizability, molar refractivity, dielectric constants of europium doped and for alkaline earth ion variation were calculated and are listed in the Table 2(a) & 2(b), respectively.

From the Table 2 (a), the increasing values of density with the concentration of europium oxide is because of the substitution of ZnO (d=5.16 g/cc) with the Eu_2O_3 element (d=7.40 g/cc) in the network [15]. It reveals more tightness of the glass structure. The crowding of the glass matrix by europium interstices reduces the distance among rare earth and oxygen ions [16]. The increase in the refractive index (n) with the Eu^{3+} ion content is mostly expected to generate more ionic dipoles when being exposed to an electric field [17].

Table 2 (a): Physical Characteristics of Eu^{3+}: SZB Glasses

Physical Parameters	SZB:Eu^{3+}		
	1 Mol%	2 Mol%	3 Mol%
Density (gm / cc)	3.24	3.29	3.37
Molar Volume V_m (cm^3)	24.4	24.8	25.0
Refractive Index (n)	1.55	1.56	1.57
Conc. Of Eu ion (cm^{-3})	2.46	4.84	7.20
Polaron radius γ_p (A^0)	6.42	5.13	4.49
Inter nuclear distance γ_i (A^0)	15.9	12.7	11.1
Field strength F (10^{15}) (cm^{-2})	0.72	1.13	1.48
Polarizability α_e (10^{-24}) (cm^3)	3.12	3.23	3.27
Dielectric constant (ε)	2.42	2.46	2.47
Reflection loss R (%)	2.45	2.54	2.56
1- (R_m / V_m) = M	0.68	0.67	0.67

Table 2 (b): Physical Characteristics of Host (Alkaline Earth) Variation of Eu^{3+}: MZB Glasses

Physical Parameters	Eu^{3+}: MZB (M=Ca, Sr, Ba) (1 mol %)		
	CaO	SrO	BaO
Density (gm / cc)	3.12	3.24	3.2
Molar Volume V_m (cm^3)	25.2	24.4	27.0
Refractive Index (n)	1.53	1.55	1.57
Conc. Of Eu ion (cm^{-3})	2.38	2.46	2.22
Polaron radius γ_p (A^0)	6.50	6.42	6.64
Inter nuclear distance γ_i (A^0)	16.1	15.9	16.4
Field strength F (10^{15}) cm^{-2}	0.70	0.72	0.67
Polarizability α_e (10^{-24}) (cm^3)	3.23	3.12	3.27
Dielectric constant (ε)	2.35	2.42	2.47
Reflection loss R (%)	2.28	2.45	2.56
1- (R_m / V_m) = M	0.69	0.68	0.67

We observe from Table 2(b), when ionic radius of M^{2+} changes in the host matrix from $Ca^{2+}\rightarrow Sr^{2+}\rightarrow Ba^{2+}$, the 'n' value of the system increases. The density also increases with the molar weight of cation variation. The change of molar volume with the substitution of an alkaline earth ion may attribute to increase of ion size. The metallization factor of the glass is much less than one, indicating the insulating nature [18].

Structural Analysis

Figure 1 shows the characteristic X-ray pattern for a europium doped SZB glasses, and also composition variation in the host matrix. Both patterns show a broad bump at lower angles, confirmed the glassy nature of the sample [3].

Infrared spectra of Eu^{3+}:MZB glasses usually have several broad and moderate bandwidth peaks due to the bridging oxygen vibrations like stretching (~800-1200cm^{-1}& 600–800cm^{-1}) and bending (~ 600–500cm^{-1}& 500–400cm^{-1}) [19]. Figure 2 shows the FT-IR spectra of Eu^{3+} (1-3 mol %) and M^{2+} (Ca^{2+}, Sr^{2+}, Ba^{2+}) ions in zinc borate glasses, recorded in 600–2000cm^{-1} range.

The FTIR spectra exhibited four broad absorption band regions, which are stretching and bending of bridging oxygen atoms. The peaks at around 420-425 cm^{-1} are of stretching of ZnO_4 units [20]. In order to notice the effect of the alkali addition on the structure of borate network, we look in the mid infrared region, bands in between 441- 457 cm^{-1} are due to stretching of metal ions like Ba^{2+}& Sr^{2+} [21]. The moderately broad band at around 689-702 cm^{-1} can be allocated to B-O-B bending vibrations of bridging oxygen between trigonal boron [3]. The vibrations of boron with non bridging oxygen atoms in BO_4 unit results the wide peak at 1050 cm^{-1}[22]. The band at 1243 cm^{-1} was expected to be of B-O asymmetric stretching vibrations from pyro to ortho groups in BO_3 units [20].

The peak at 415 cm^{-1} owes the manifestation of Eu-O bond [23]. Slight modifications in the IR pattern were observed by the change of dopant concentration as well as alkaline variation.

These assignments are well agreed with the other borate glasses [3, 20-23] listed in the Table 3. The positions of bands are slightly approaching the higher wave number side due to incrin addition to the change of mass of network modifier (Zn).

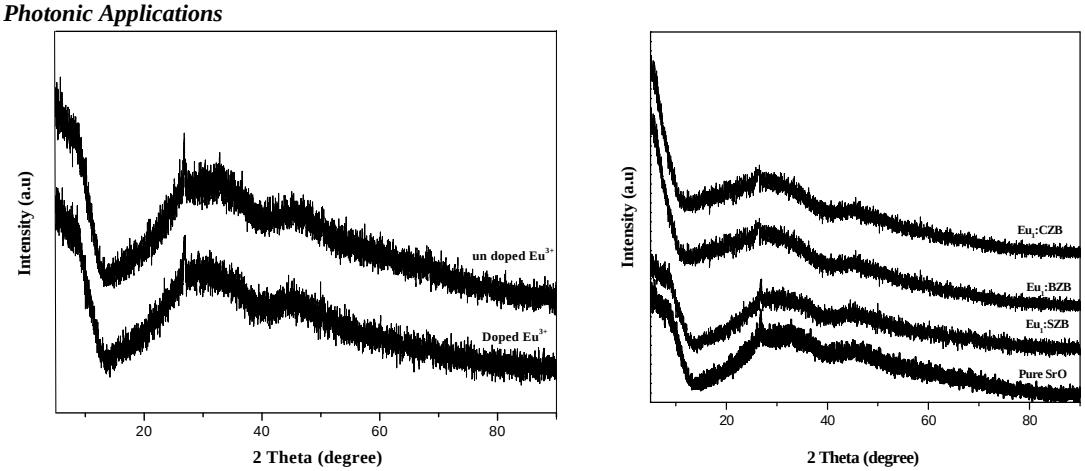

Figure 1: XRD Pattern of Pure and Europium Doped MZB Glasses

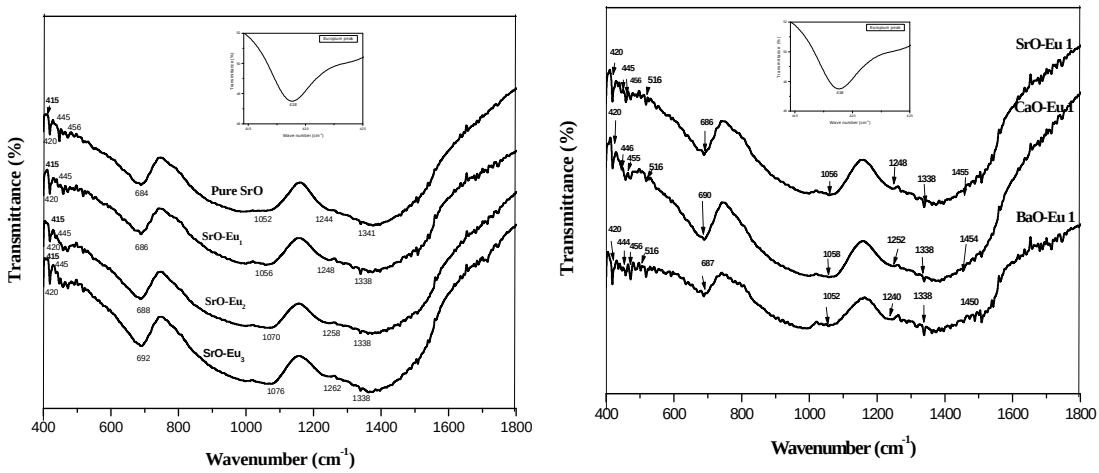

Figure 2: FTIR Spectrum of (a) Eu^{3+}: SZB (b) Eu^{3+}: MZB Oxide Ions in Zinc Borate Glasses

Table 3: FTIR Band Assignments of Eu3+ (Mol %) Doped MZB & SZB Glasses

Sample	Eu^{3+}	Znmetal Ion	MZB	Bending of B-O-B	B-O Stretching of BO_4 Units	Asymmetric Stretching of BO_3	Stretching of NBO
CZB:Eu_1	415	420		690	1058	1252	1338
SZB:Eu_1	415	420		686	1056	1248	1338
BZB:Eu_1	415	420		687	1052	1240	1338
			443-454				
SZB:Eu_1	415	420		686	1056	1248	1338
SZB:Eu_2	415	420		688	1070	1258	1338
SZB:Eu_3	415	420		692	1076	1262	1338
Reference	[23]	[20]	[21]	[03]	[22]	[21]	[23]

Absorption Spectral Analysis

The absorption spectra of the Eu^{3+} doped MZB glasses are reported in the range 300-2400nm. Optical Bands in the Spectra are because of inhomogeneous broadening 4f- 4f optical excitations from the ground to their corresponding excited states of Eu^{3+} Ions. Figure 3 shows optical spectra along with their band assignments of different europium concentrations and Figure 4, different alkaline earth Ions in the UV-VIS-NIR region.

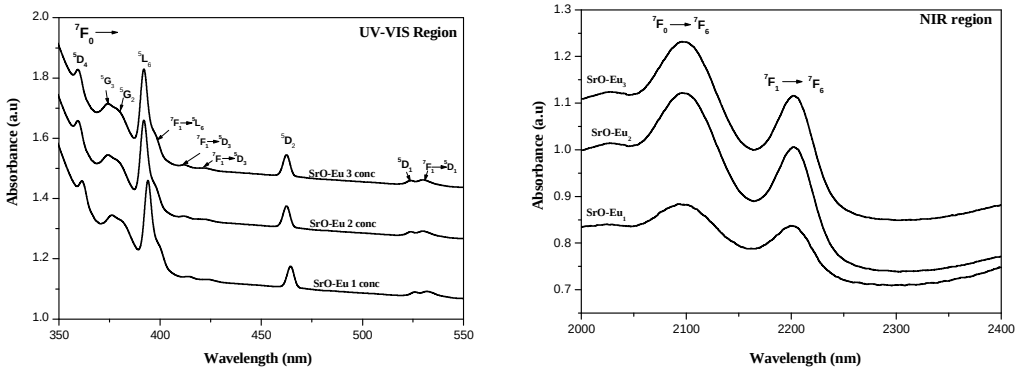

Figure 3: Absorption Spectra of Europium Doped SZB Glasses In (a) UV-VIS (b) NIR Regions

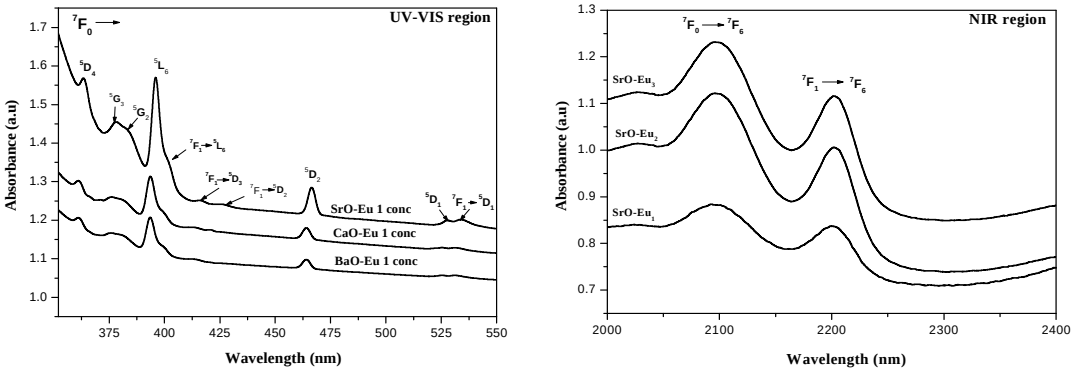

Figure 4: Absorption Spectra of Europium Doped Different MZB Oxide Ions in Zinc Borate Glass in (a) UV-VIS (b) NIR Regions

Figure 5: Digital Photograph of Eu^{3+} Ion Doped SZB Glasses (a) Under Daylight (b) Under UV Light

From the spectrum, 12 transition bands observed, out of which, 10 are in UV-VIS and 2 in the NIR region. The peaks correspond to $^7F_0 \rightarrow {}^5D_1$, $^5D_2$, $^5L_6$, $^5G_2$, $^5G_3$, $^5G_5$, $^5D_4$ and $^7F_1 \rightarrow {}^5D_1$, $^5D_3$, $^5L_6$in UV-Vis region and $^7F_{0,1} \rightarrow {}^7F_6$ in the NIR region [1]. Among all transitions, the spin forbidden transitions $F_J \rightarrow D_J$ are very weak [3] and the transition $^7F_0 \rightarrow {}^5D_2$ is more acute than $^7F_0 \rightarrow {}^5D_1$transition. Although the transition $^7F_0 \rightarrow {}^5L_6$ is forbidden by ΔS and ΔL, but allowed by ΔJ selection rule, it was more intense than other transitions. The peak $^7F_0 \rightarrow {}^5D_3$ in the spectra is not observed as it is a spin forbidden **[**3]. The positions of $^7F_0 \rightarrow {}^7F_6$ and$^7F_1 \rightarrow {}^7F_6$peaks reveal the energy gap, which is comparable to otherEu^{3+} doped glasses. This small energy gap results the population of $^7F_1$ and $^7F_0$ states [2]. Figure 5 (a) shows the prepared glass sample in white color when it is under daylight and Figure 5 (b) shows an extreme red emission under UV radiation, specifies the characteristic of the Eu^{3+} ion in the system.

Optical Band Gap (E_{opt}), Urbach Energy (ΔE) and Optical Basicity

Optical band gap has been computed for analysis optically induced transitions, conductivity of a solid material [1] and glass structure. For Eu^{3+} doped and different alkaline earth ions in zinc borate glasses, the optically induced transitions are calculated from the optical spectra. The band gap graphs for Eu^{3+}: SZB and Eu^{3+}: MZB were shown in Figure 6 (a) & (b) and calculated values are tabulated in Table 4

We observed the direct transition values as 2.37, 2.76, 3.07 eV and for indirect 2.82, 3.00, 3.37 eV with dopant ion concentration from 1-3 mol %. The increase in the band gap values with Eu^{3+} ion results the lower of non bridging oxygen formation, leads to structural variations in the host glass. So, oxide ion polarizability is the cause of alterations in the band gap. Further, it increases the donor facilities there, by enhancement of the localization of electrons in the host matrix. Also, we observe the values from Ca, Sr to Ba as 4.00, 3.55, 4.31 eV and 2.37, 2.93, 3.11 eV for direct and indirect transitions respectively. This is due to the existence of various alkaline earth ions in the host matrix.

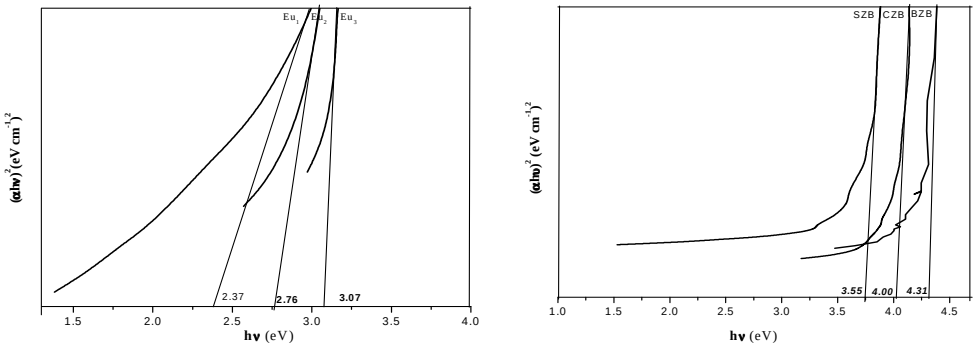

Figure 6 (a): The Tauc's Plots For $(Ahυ)^2$ vs Hυ for Direct Band Gap Energy for Different Conc. of Eu^{3+} & Mzb Oxide Ions in Zb Glasses

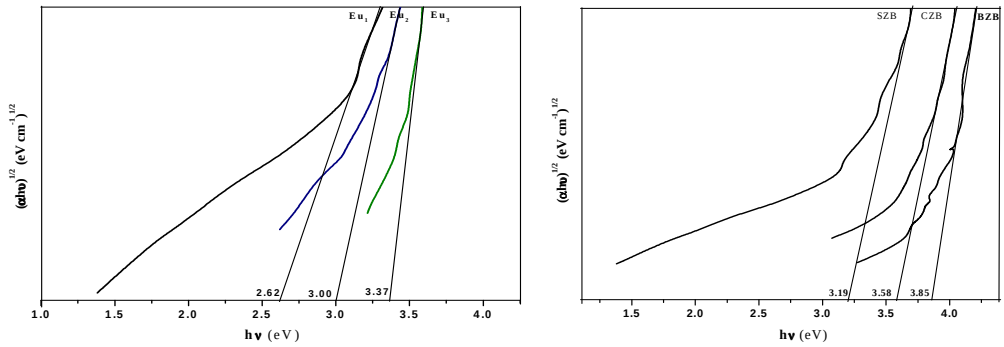

Figure 6 (b): The Tauc's Plots Drawn for $(Ahυ)^{1/2}$ Vs Hυ for Indirect Band Gap Energy for Different Conc. of Eu^{3+} & Mzb Oxide Ions in Zb Glasses

Table 4: Optical Band Gap (Ev), Urbach, Optical Basicity of Eu^{3+}: Szb & Eu^{3+}: Mzb Glasses

Glass System	Direct	Indirect	Urbach	Optical Basicity
SZB-Eu_1	2.37	2.83	0.29	0.636
SZB-Eu_2	2.76	3.35	0.38	0.646
SZB-Eu_3	3.07	3.55	0.72	0.652
CZB-Eu_1	4.00	2.37	0.61	0.631
SZB-Eu_1	3.55	2.93	0.29	0.636
BZB-Eu_1	4.31	3.11	0.42	0.644

Table 5: Absorption Transitions, Experimental & Calculated Oscillator Strengths ($\times 10^{-6}$) for Eu^{3+}: MZB &Eu^{3+}: SZB Glasses

$^7F_0 \rightarrow {}^5D_4$	27700	0.13	0.129	0.106	0.105	0.152	0.147	0.116	0.155	0.166	0.165
$^7F_0 \rightarrow {}^5G_4$	26666	0.033	0.079	0.178	0.065	0.038	0.090	0.091	0.095	0.102	0.101
$^7F_0 \rightarrow {}^5G_2$	26315	0.260	0.203	0.197	0.186	0.201	0.126	0.112	0.259	0.36	0.32
$^7F_0 \rightarrow {}^5L_6$	25445	0.946	0.697	0.544	0.905	0.434	0.805	1.081	0.801	1.47	0.79
$^7F_1 \rightarrow {}^5L_6$	25000	0.052	0.132	0.234	0.172	0.130	0.153	0.094	0.152	0.111	0.150
$^7F_1 \rightarrow {}^5D_3$	24154	0.043	0.082	0.514	0.715	0.113	0.072	0.269	0.102	0.063	0.119
$^7F_1 \rightarrow {}^5D_2$	21598	0.222	0.221	0.204	0.203	0.188	0.138	0.284	0.283	0.357	0.356
$^7F_0 \rightarrow {}^5D_1$	19047	0.017	0	0.013	0	0.035	0	0.038	0	0.019	0
$^7F_1 \rightarrow {}^5D_1$	18832	0.264	0.209	0.177	0.192	0.103	0.131	0.169	0.267	0.378	0.336
$^7F_0 \rightarrow {}^5F_6$	4773	2.23	1.54	1.59	1.58	1.42	1.41	0.993	1.405	1.392	1.39
$^7F_1 \rightarrow {}^5F_6$	4543	1.21	1.27	1.00	1.31	1.29	1.17	0.661	1.16	1.212	1.147
		δrms = 0.050 β = 0.9966 δ = 0.341		δrms = 0.026 β = 0.9964 δ = 0.353		δrms = 0.015 β = 0.9957 δ = 0.431		δrms = 0.039 β = 0.9956 δ = 0.441		δrms = 0.043 β = 0.9953 δ = 0.472	

Table 6: The Judd-Ofelt Parameters ($\Omega_\lambda \times 10^{-20}$) for Eu^{3+}: MZB glasses

Host matrix	J-O Parameters			Trend	Spectroscopic quality Factor $\chi = \Omega_4 / \Omega_6$
	Ω_2	Ω_4	Ω_6		
CZB-Eu_1	8.64	2.87	1.19	$\Omega_2 > \Omega_4 > \Omega_6$	2.41 Present work
SZB-Eu_1	5.31	3.2 2.27	1.35	$\Omega_2 > \Omega_4 > \Omega_6$	2.37 Present work
BZB-Eu_1	7.71	3.47	1.50	$\Omega_2 > \Omega_4 > \Omega_6$	1.5 Present work
Reported Glass systems	5.61	1.09	2.61	$\Omega_2 > \Omega_4 > \Omega_6$	1.32 [28]
	2.90	3.90	0.98	$\Omega_2 > \Omega_4 > \Omega_6$	1.11 [29]
	8.19	3.35	1.89	$\Omega_2 > \Omega_4 > \Omega_6$	2.06 [30]
	8.77	4.13	1.78	$\Omega_2 > \Omega_4 > \Omega_6$	1.88 [30]
	6.44		1.44	$\Omega_2 > \Omega_4 > \Omega_6$	2.86 [31]

Urbach energy is a measure of a degree of irregularity in amorphous solids. The values from Table 4 both in europium ion variation and alkaline earth ion replacement imply the presence of fewer defects within the titled glass [10]. The capacity to donate the negative charge to the probe ion is basically predicted from its chemical composition and basicity moderating parameters of the cations inside the system [24]. The increase of optical basicity is observed with dopant ion concentration and the replacement from $Ca^{2+} \rightarrow Sr^{2+} \rightarrow Ba^{2+}$ in the host matrix. It concluded the development of bonds with improved covalence in the sample structure.

Oscillator Strengths

Oscillator strengths are used to know the facts about intensities of an absorption bands. The oscillator strength values were determined using the expressions given by [25,26]. The results of both europium ion concentration variations and alkaline earth ion variations in the host matrix in Table 5 clearly shows the dependence oscillatory strength (*f*) values on the composition of the glass matrix and the spin forbidden transition $^7F_1 \rightarrow {}^5D_1$ intensity. The narrow root means square variation (δ_{rms}) indicates the accuracy among experimental and calculated intensity parameters

Judd-Ofelt Analysis

The structure around the RE^{3+} ion site and nature of a dopant ion with its neighboring ligand ions was known from J-O parameters. There are two methods to evaluate the reduced square matrix elements□□U□□□^{2}(where λ=2,4,6) [2].

Evaluation of Parameters from the Absorption Spectra

The assessment of J-O parameters is a little bit difficult for the europium ion, as we observe transitions like $^5D_1$, $^5D_2$ and $^5L_6$ only from $^7F_{0,1}$ ground states with preferable intensity in the absorption spectrum. The calculated J-O values for different alkaline earth oxide ion replacement in the host matrix are tabulated and compared [28-31] in Table 6. It follows the bias i. e. $\Omega_2>\Omega_4>\Omega_6$. The existence of strong covalence among the Eu^{3+} and its surrounding ligands are proved from larger Ω_2 values and also confirmed from the bonding parameter (δ) and intensity ratio [1

Evaluation of Parameters from the Emission Spectra

Figure 7 shows the emission spectra of the Eu^{3+}: SZB and $Eu^{3+:}$ MZB glasses, recorded at room temperature by exciting the sample at 393 nm. It consists of five transitions, $^5D_0\rightarrow{}^7F_0$, $^5D_0\rightarrow{}^7F_1$,$^5D_0\rightarrow{}^7F_2$,$^5D_0\rightarrow{}^7F_3$ and $^5D_0\rightarrow{}^7F_4$ respectively. Using emission transitions $^5D_0\rightarrow{}^7F_{2,4,6}$ J-O intensity parameters had been determined because the transitions $^5D_0\rightarrow{}^7F_{2,4,6}$ depend on the Ω_λ (λ=2,4,6) values while the transition $^5D_0\rightarrow{}^7F_1$ is host independent. The presence of non-degenerate transition $^5D_0\rightarrow{}^7F_0$ in the emission spectra confirms the higher asymmetry among the Eu^{3+} and its surrounding ligands. It also indicates Eu^{3+} ions are in a good polarizable chemical structure [27]. J-O parameter values are compared with other stated glasses [28-31] are listed in the Table 6.

Radiative Properties

Radiative properties for europium ion concentrations and different alkaline earth oxides have been calculated with the help of JO parameters of the emission characteristics for the Eu^{3+}: MZB glasses. The transition probability (A_R) from an initial state ΨJ to a final state Ψ^1J^1 is calculated [32]. The radiative branching ratio (β_R), stimulated emission cross section (σ_e), gain band width & radiative lifetime (τ_R) were calculated using radiative transition probability value, making use of the relation given by Ait Hana et al [33] and are tabulated in Table 7.

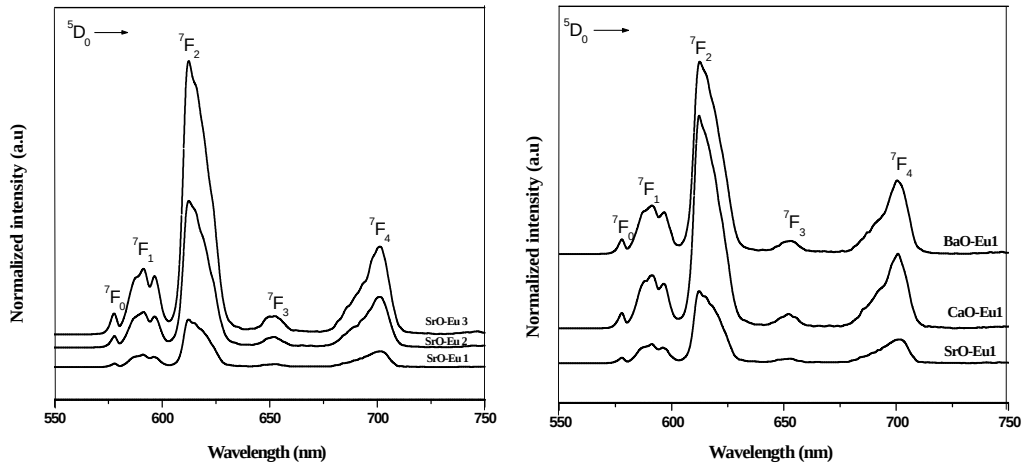

Figure 7: Emission Spectra of (a) Eu^{3+}: SZB and Eu^{3+}: MZB Oxide Ions in Zinc Borate Glasses

Table 7: Radiative Properties for the Eu^{3+}: MZB and Eu^{3+}: SZB Glass

System	Level	Λp	Δλp	A_r	Bm	B_r	Σ_e (10^{22})	Gain Band Width (10^{25}) Cm^3	Lifetime
BZB-Eu_1	$^5D_0 \rightarrow {}^7F_0$ $^5D_0 \rightarrow {}^7F_1$ $^5D_0 \rightarrow {}^7F_2$ $^5D_0$ $\rightarrow {}^7F_3$ $^5D_0 \rightarrow {}^7F_4$	578 591 612 652 700	2.96 13.80 18.41 12.32 9.99	0 50.33 179.6 0 38.21	0.004 0.120 0.700 0.024 0.148	0 0.1877 0.669 0 0.1425	0 16.05 37.33 0 8.55	22.1 68.7 8.5	A_T = 2.68 mS τ_R = 3.72 mS
CZB-Eu_1	$^5D_0 \rightarrow {}^7F_0$ $^5D_0 \rightarrow {}^7F_1$ $^5D_0 \rightarrow {}^7F_2$ $^5D_0 \rightarrow {}^7F_3$ $^5D_0 \rightarrow {}^7F_4$	578 591 612 652 700	2.22 14.50 13.27 11.1 11.22	0 51.2 189.3 0 44.5	0.004 0.155 0.623 0.027 0.189	0 0.179 0.80 0 0.190	0 16.34 57.4 0 9.27	23.6 6.1 10.4	A_T = 2.85 mS τ_R = 3.50 mS
SZB-Eu_1	$^5D_0 \rightarrow {}^7F_0$ $^5D_0 \rightarrow {}^7F_1$ $^5D_0 \rightarrow {}^7F_2$ $^5D_0$ $\rightarrow {}^7F_3$ $^5D_0 \rightarrow {}^7F_4$	578 591 612 652 700	3.7 13.8 13.58 11.84 16.28	0 50.22 186.8 0 52.2	0.007 0.149 0.593 0.022 0.226	0 0.173 0.78 0 0.21	0 16.84 55.3 0 7.49	23.2 75.09 12.2	A_T = 2.89 mS τ_R = 3.45 mS
SZB-Eu_2	$^5D_0 \rightarrow {}^7F_0$ $^5D_0 \rightarrow {}^7F_1$ $^5D_0 \rightarrow {}^7F_2$ $^5D_0$ $\rightarrow {}^7F_3$ $^5D_0 \rightarrow {}^7F_4$	578 591 612 652 700	2.77 13.90 15.80 12.15 13.48	0 51.02 187.9 0 56.03	0.005 0.122 0.669 0.024 0.177	0 0.172 0.76 0 0.23	0 16.55 46.40 0 9.42	3.0 73.3 12.6	A_T = 2.94 mS τ_R = 3.39 mS
SZB-Eu_3	$^5D_0 \rightarrow {}^7F_0$ $^5D_0 \rightarrow {}^7F_1$ $^5D_0 \rightarrow {}^7F_2$ $^5D_0 \rightarrow {}^7F_3$ $^5D_0 \rightarrow {}^7F_4$	578 591 612 652 700	2.51 14.61 16.63 12.32 11.71	0 50.05 189.40 0 59.7	0.011 0.095 0.698 0.029 0.165	0 0.167 0.757 0 0.242	0 15.67 44.43 0 11.55	22.9 73.88 13.52	A_T = 2.99 mS τ_R = 3.34 mS

The radiative probability for transition $^5D_0 \rightarrow {}^7F_2$ found to be 186.8, 187.9 and 189.4 corresponding to Eu_1: SZB, Eu_2: SZB, Eu_3: SZB and 179.6, 189.3 and 186.8, for Eu_1: BZB, Eu_1: CZB, Eu_1: SZB, respectively. The experimental branching ratio values for all follow $^5D_0 \rightarrow {}^7F_2 > {}^7F_1 > {}^7F_4 > {}^7F_3$.

The stimulated emission cross section is much larger in magnitude for transition $^5D_0 \rightarrow {}^7F_2$ and the measured branching ratio are 70, 62, 59 % for BZB, CZB, SZB glasses respectively in MZB glasses suggest that $^5D_0 \rightarrow {}^7F_2$ is vigorous and there through suggesting that the present glass best for the laser [34]. The higher values of A_R, σ_e, β_m indicates the $^5D_0 \rightarrow {}^7F_2$ emission line in Eu^{3+}: MZB glass exhibits extreme red fluorescence.

Excitation and Emission Spectra

The photoluminescence characterization is beneficial for review of optical characteristics of the samples. Figure 8 indicates excitation spectra of different europium concentrations in SZB glasses and europium doped different alkaline earth oxides in ZB glasses. The sharp peaks are because of intra 4*f* transitions of Eu^{3+} ions. These transitions are observed to increase with Eu^{3+} ion concentration. The same is observed in ZnO phosphor glasses containing Eu^{2+}, Eu^{3+} ions [34]. No substantial change in band positions with host variation confirms crystal field splitting. In an excitation spectrum, among 6 bands, the eminent $F_0 \rightarrow L_6$ excitation band has been most appropriate to estimate the emission spectrum of Eu^{3+} glass [14].

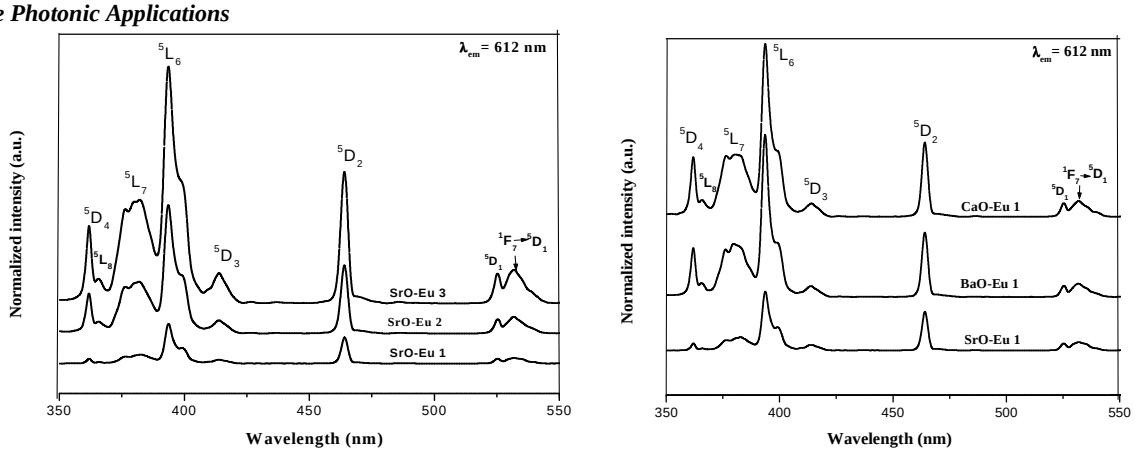

Figure 8: Excitation Spectra of (a) Eu^{3+} Ion Doped SZB (b) Different MZB Oxide Ions in Zinc Borate Glasses

The $^5D_0 \rightarrow {}^7F_1$ transition belongs to magnetic dipole and could be useful to the estimation of transition probabilities of excited levels and independent of crystal field strength [35]. The peak $^5D_0 \rightarrow {}^7F_2$ is due to electric dipole, indicating that Eu^{3+} ions are not in the symmetry center of the host matrix. The known fact is that Eu^{3+} ions occupy the substitution sites of Zn^{2+} ions permitting$^5D_0 \rightarrow {}^7F_1$, $^5D_0 \rightarrow {}^7F_2$ transitions, is due to having the same total angular momentum [9, 36]. Among 5 observed emission bands, $^5D_0 \rightarrow {}^7F_2$ transition has shown bright red emission and this hypersensitive transition following $\Delta J=2$ selection rule. Because of J-mixing effect among multiplets, the transition $^5D_0 \rightarrow {}^7F_3$ has low intensity [14].

Asymmetry ratio(R) specifies the surroundings around the RE^{3+} ion sites and the covalence of RE-O bonds [37]. The variation of intensity ratio values of the prepared system along with stated glasses [38-41] for comparison is listed in Table 8. The increasing intensity ratio values confirm an extent covalence around Eu-O bonds.

Table 8: Intensity Ratio Values of Present System and Other Reported Glasses

Glass Matrix	Intensity Ratio (R)
SZB-Eu1	3.97
CZB-Eu_1	4.00
BZB-Eu_1	5.79
SZB-Eu_2	5.46
SZB-Eu_3	7.30
ZnPbBEu10 [38]	3.89
TZWEu10 [39]	5.1
Al_2O_3 [40]	4.00
$CaMoO_4$ [41]	7.50

Decay Analysis

Decay analysis gives additional information of fluorescence propertiesfor$^5D_0 \rightarrow {}^7F_2$. From Fig.9, clearly all curves exhibited a single exponential behavior with a lifetime of 2.43, 2.44, 2.39 ms corresponding to Eu_1: SZB, Eu_2: SZB, Eu_3: SZB and 2.49, 2.46, 2.43 ms to Eu_1: BZB, Eu_1: CZB, Eu_1: SZB, respectively.

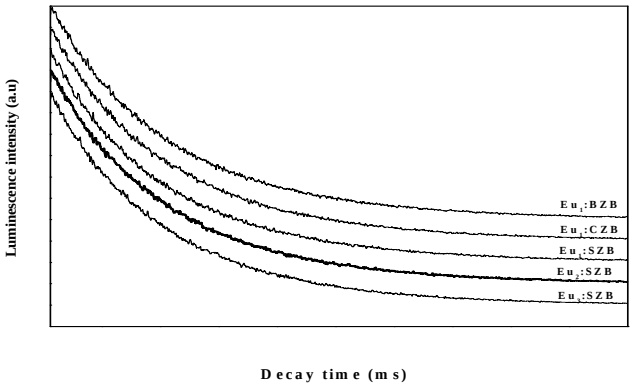

Figure 9: Decay Curves of Eu^{3+} Ion Concentration Dependent Eu^{3+}: SZB & Eu^{3+}: MZB Glasses

The values are listed in Table 9 and are observed to be slight lower than the other glasses like Fluoride phosphate [42], EPbFB [43], LLiFB [2], LiABP:Eu [44]. The radiative lifetimes evaluated from J-O theory are 3.45, 3.39 and 3.34 ms for Eu_1: SZB, Eu_2: SZB, Eu_3: SZB and 3.73, 3.50, 3.45 ms for Eu_1: BZB, Eu_1: CZB, Eu_1: SZB, respectively. The lower experimental lifetime than calculated in both the cases is due to non-radiative relaxation of $^5D_0 \rightarrow {}^7F_2$ level. The non-radiative transition is because of interaction between dopant and host matrix resulting the emission of multi phonon, called as the multi phonon's relaxation (W_{MPR}) process and radiative transition was due to ion-ion interaction amongEu^{3+} ions, including emission transitions.

From Table 9, the calculated W_{MPR} found to be 121,114, and 117 sec^{-1} for Eu_1: SZB, Eu_2: SZB, Eu_3: SZB and 132,120,121 sec^{-1} for Eu_1: BZB, Eu_1: CZB, Eu_1: SZB glasses. The small magnitudes in W_{MPR} are due to small deviations in τ_m and τ_R values and the quantum efficiency (ŋ) was found to be greater than 70% for the Eu^{3+}: MZB system, due to the non existence of multi phonon's relaxation, cross-relaxation from $^5D_0$ level.

Table 9: Amplification Parameters for the $^5D_0$ Level of Eu^{3+}: SZB and Eu^{3+}: MZB Glasses

SZB:Eu &MZB:	$Eu\tau_R$ (ms)	τ_m (ms)	W_{MRP} (sec)	ŋ %
SZB: Eu_1	2.430	3.45	121	70
SZB: Eu_2	2.444	3.39	114	72
SZB: Eu_3	2.399	3.34	117	72
$BZBEu_1$	2.496	3.73	132	67
$CZBEu_1$	2.465	3.50	120	70
$SZBEu_1$	2.430	3.45	121	70
Reported Systems				
Fluoride phosphate [42]	2.30	3.9	178	60
EPbFB [43]	1.60	2.52	226	64
LLiFB [02]	1.34	1.75	175	77
LiABP:Eu3+ [44]	3.49	6.46	132	54

CIE color Chromaticity Coordinates

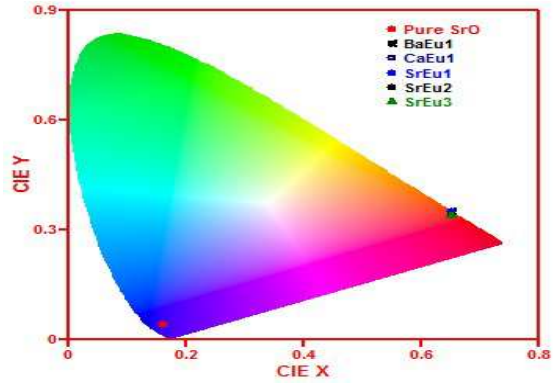

Figure 10: CIE Chromaticity diagram for Eu^{3+} ions in MZB Glasses

CIE diagram is appropriate to determine the emission color of the organized glass. The color coordinates of the luminescence are calculated by adopting the technique observed via Vijaya Kumar et al [45]. Figure 10 shows the color coordinates of the Eu^{3+}: MZB excited at 393nm determined from the interrelated emission spectra (Figure 7).

CONCLUSIONS

- The increasing value of density affirms the close packed glass structure.
- IR data revealed the rearrangement of a borate frame network, causing a change of boron coordinates from BO_4 to BO_3 units.
- The peaks in the UV-Visible spectra reveal the dependence of nature of a doping ion.
- The observed peak variations in PL graph indicates that the wave length of excitation depends purely on the material composition when the sample is doped with a rare earth element.
- From Ω_2 parameter proves hypersensitive behavior of $^5D_0 \rightarrow {}^7F_2$ transition, confirms Eu^{3+} ions are situated in a deeply polarizable chemical domain.
- The high luminescence intensity ratio R specifies lower symmetry around Eu ions and higher Eu-O covalence.
- The values of A_R, σ_e, β_m indicates the $^5D_0 \rightarrow {}^7F_2$ emission line is best for the development of color display devices and visible red laser.
- Among the alkaline earth modifiers, strontium was found to be best for enhancing the lifetime of $^5D_0$ level in the borate glass matrix.
- CIE diagram confirms the present titled glass system was best for laser applications.
- From above results, the europium doped MZB glass system is best for photonic applications.

REFERENCES

1. *S. Hima Bindu, Ch. Linga Raju, Et Al. Optical Materials, 62 (2016) 655–665.*
2. *B. Deva Prasad Raju, C. Madhukar Reddy, Et Al. Optical Materials, 34 (2012) 1251–1260.*
3. *K. Marimuttu, C. K. Jaya Shankar, Physica Status Solidi A, 206 (2009)131–139.*

4. *K. Marimuttu, C. K. Jaya Shankar, Et Al. Solid State Sciences, 11 (2009) 1297–1302.*
5. *D. E. Day, J. Non-Crystal Solids, 21 (1976) 343–372.*
6. *Ramesh Boda, G. Srinivas, IOSR-JAP, 7 (2015) 27–34.*
7. *G. Krishna Kumari, R. V. S. S. N. Ravi Kumar, Materials Research Bulletin, 47 (2012) 2646–2654.*
8. *H. Yamasaki, K. Minato, Solid State Ionic, 172 (2004) 349–352.*
9. *Te Hua Fang, Walter Water, J. Phys. Chem. Solids, 70 (2009) 1015–1018.*
10. *R. Vijaya Kumar, K. Marimuttu, Et Al. J. Luminescence, 154 (2014) 160–167.*
11. *Priya Murugasen, Deepa Shajan, IJPS, 10 (2015) 554–561.*
12. *N. Vijaya, C. K. Jaya Shankar, J. Molecular Structure, 1036 (2012) 42–50.*
13. *S. Lakshimi Srinivasa Rao, Md. Shareefuddin, IJEST, 4 (2012) 25–35.*
14. *M. Venkateswarulu, B. H. Rudramadevi, IJCRGG, 7 (2015) 607–612.*
15. *A. Cha Line, J. L. Pascal, Material Letters, 58(2004)2776–2780.*
16. *R. S. Gedam and D. D. Ramteke, J. Rare Earths, 30 (2012) 785–789.*
17. *S. A. Reduan, S. Hashim, Z. Ibrahim, N. Tamchek, J. Molecular Structure,1060 (2014) 6–10.*
18. *Betigeri, A. S., & Dixit, M. A. N. A. S. I. (2014). Modification in Human Face Image for Personal Identification. International Journal of Applied Engineering Research and Development, 4(2), 13–22.*
19. *Akshathawagh, Raviprakash. Y, International Journal of Technical Research & Applications, 23 (2015) 39-45.*
20. *Fei Wang, A. Stamboulis, Key Engineering. Materials, 361 (2008) 825–828.*
21. *Manisha Pal, Baishakhi Roy, Et Al. Journal of Modern Physics, 2 (2011) 1062–1066.*
22. *Avadhesh Kumar Yadav, C R Gautam, Indian Journal of Pure & Applied Physics, 53 (2015) 42–48.*
23. *S. Radha, E. M. Culea, J. Chemical Physics Letters, 460 (2008) 196–199.*
24. *K. Annapurna, S. Buddudu, Et Al. J. Molecular Structure, 741 (2005) 53–60.*
25. *B. Sumalatha, Ch. Linga Raju, Et Al. J. Molecular Structure, 1006(2011) 96–103.*
26. *B. R. Judd, Phys. Rev. B, 127 (1962) 750–761.*
27. *G. S. Ofelt, J. Chem. Phys, 37 (1962) 511–520.*
28. *H. F. Brito, J. F. S. Menezes, J. Alloys Compounds, 275 (1998) 254–257.*
29. *S. Hazarika, S. Rai, Optical Materials, 27 (2004) 173–179.*
30. *B. C. Jamalaih, J. Suresh Kumar, J. Alloys Compounds, 478 (2009) 63–67.*
31. *K. Upendra, C. K. Jaya Sankar, J. Optics Communication, 284(2011) 2909–2914.*
32. *F. Fermi, M. Bettinelli, Inorg. Chim. Acta, 163 (1988) 123–125.*
33. *Pavani Krishnapuram, Suresh Kumar Jakka, J. Molecular Structure, 1028 (2012) 170–175.*

34. *Hsiao, M. K. (2013). Current Sustainability Marketing and Communications Effect to Consumers Attitude to Purchase Sustainable Products. International Journal of Research in Business Management, 1(2), 45–54.*
35. *N. Ait Hana, M. Taibi, J. Mater. Environ. Sci, 5 (2014) 2000–2007.*
36. *C. Panatarani, K. Okuyama, J. Phys. Chem. Solids, 65 (2004) 1843–1847.*
37. *P. Rehana, B. Deva Prasad Raju, Et Al. Advanced Material letters, 7 (2016) 170–176.*
38. *G. Blasse, B. C. Grabmaier, Luminescence Materials, New York 1994.*
39. *R. Vijayakumar, K. Marimuttu, Et Al. J. Luminescence, 154 (2014) 160–167.*
40. *J. A. Capobianco, P. P Proulx, Phys. Rev. B, 42 (1990) 5936–5944.*
41. *Y. Gandhi, N. Veeraiah, J. Alloys Compounds, 508 (2010) 278–291.*
42. *N. Rakov, G. S. Maciel, J. Luminescence, 127 (2007) 703–706.*
43. *A. K. Parchur, R. S. Ningthoujam, Dalton Trans, 40 (2011) 7595–7601.*
44. *H. E. Heidepriem, D. Ehrt, J. Non-Crystalline Solids, 208 (1996) 205–216.*
45. *S. Arun Kumar, K. Marimuttu, Physica B, 416 (2013) 88–100.*
46. *Cicek, V. O. L. K. A. N., & Ozdemir, M. E. H. M. E. T. (1). Characterization Studies of Aqueous Immersion Solutions Of Novel Environmentally Friendly Organometallic Corrosion Inhibitors Used to Cure Aluminum 2024, 6061, AND 7075 Alloys Substrates In Corrosive Media. International J. of General Engineering and Technology (IJGET), 2 (2), 1, 16.*
47. *K. Linganna, C. K. Jayasankar, Spectro. Chem. Acta Part A: Molec. Biomol. Spectro, 97(2012)788!–797.*
48. *M. Vijaya Kumar, K. Marimuthu, Et Al. Optical Materials, 37 (2014) 695–705.*